Pergamon

Geochimica et Cosmochimica Acta, Vol. 68, No. 3, pp. 547–556, 2004

0016-7037/04 $30.00 + .00

doi:10.1016/S0016-7037(00)00444-7

# Capture of molybdenum in pyrite-forming sediments: Role of ligand-induced reduction by polysulfides

TRENT P. VORLICEK,† MANI D. KAHN, YASUHIRO KASUYA, and GEORGE R. HELZ*
Department of Chemistry and Biochemistry, University of Maryland, College Park, MD 20742, USA

(*Received January* 21, 2003; *accepted in revised form June* 20, 2003)

**Abstract**—Capture of Mo by $FeS_2$ is an important sink for marine Mo. X-ray spectroscopy has shown that Mo forms Mo-Fe-S cuboidal clusters on pyrite. Reduction of $Mo^{VI}$ must occur to stabilize these structures. Sulfide alone is a poor reductant for Mo, producing instead a series of $Mo^{VI}$ thioanions ($MoO_xS_{4-x}^{2-}$, x = 0-3). In solutions that contain both $H_2S$ and $S^0$-donors (i.e. polysulfides; dissolved $S_8$), Mo is transformed to $Mo^{IV}$ or $Mo^{V}_2$ polysulfide/sulfide anions. This intramolecular reduction requires no external reducing agent. Remarkably, an oxidizing agent ($S^0$ donor), rather than a reducing agent, stabilizes the reducible $Mo^{VI}$ complex. Thiomolybdates and their reduction products do not precipitate spontaneously; solutions supersaturated by $10^9$ with respect to molybdenite, $MoS_2$, produce no precipitate in 40 days. In 10-minute exposures, pyrite can scavenge $MoOS_3^{2-}$ and $MoS_4^{2-}$ weakly at mildly alkaline pH but can scavenge an unidentified product of the $S^0$-induced reduction of $MoOS_3^{2-}$ very strongly. On the basis of these observations, a reaction pathway for Mo capture by pyrite is proposed. Conditions that favor Mo capture by this pathway also favor pyrite growth. Ascribing Mo capture simply to low redox potential is too simplistic and neglects the likely role of oxidizing $S^0$-donors. The aqueous speciation of Mo in anoxic environments will be a function of the activity of zero-valent sulfur as well as the activity of $H_2S$(aq). 

## 1. INTRODUCTION

Enrichment of Mo in anoxic sediments and black shales is of interest because it provides information on paleoredox conditions in sedimentary environments (Dean et al., 1997, 1999; Crusius et al., 1999; Morford and Emerson, 1999; Zheng et al., 2000a,b; Yarincik et al., 2000; Adelson et al., 2001; Nameroff et al., 2002; Dellwig et al., 2002). Fully exploiting the implications of Mo enrichment requires clarification of Mo-fixing mechanisms. Marine plankton negligibly bioconcentrate $MoO_4^{2-}$, the dominant Mo species in seawater (Brumsack, 1989). Many solid surfaces, including those of clay minerals and $Fe^{III}$ or Al oxyhydroxides, sorb $MoO_4^{2-}$ only weakly at mildly alkaline pH (McKenzie, 1983; Goldberg et al., 1998). Not surprisingly, therefore, $MoO_4^{2-}$ is conservative in the oxic ocean.

Prior work in our laboratory defines conditions under which $MoO_4^{2-}$ can be transformed in sulfidic waters into thiomolybdates, $MoO_xS_{4-x}^{2-}$ (Erickson and Helz, 2000; Vorlicek and Helz, 2002). Thiomolybdates are particle-reactive (Helz et al., 1996) and probably lie in the chemical pathway leading to fixed Mo in anoxic sediments. However, much remains to be learned about this pathway. Of particular interest are interactions of sulfidized Mo species with pyrite, which is the chief Mo host-phase in anoxic sediments and black shales (Raiswell and Plant, 1980; Coveney et al., 1987; Huerta-Diaz and Morse, 1992; Dellwig, et al., 2002; Müller, 2002).

The hexavalent oxidation state of Mo is preserved during stepwise reaction of $MoO_4^{2-}$ with $H_2S$ to form $MoO_xS_{4-x}^{2-}$. Yet, Bostick et al. (2003) show that when $MoS_4^{2-}$ interacts with pyrite, Fe-Mo-S cuboidal clusters form. These structures can be stable only if Mo undergoes reduction. Known Fe-Mo-S cuboidal structures contain $Mo^{III}$ and $Mo^{IV}$ (Mascharak et al., 1983; Osterloh et al., 2000). At what stage in the scavenging of Mo by pyrite does reduction occur? What are the reducing agents and mechanism? Most importantly, if reduction is required, does Mo enrichment in sediments or in black shales imply that a critical redox threshold was reached in the sedimentary environment?

Here, we investigate the effect of zero-valent sulfur ($S^0$) on Mo chemistry in sulfidic solutions. Our results suggest that $S^0$, present in sulfidic natural waters in the form of polysulfide ions ($S_n^{2-}$) and molecular sulfur (mainly $S_8$), promotes reduction of $Mo^{VI}OS_3^{2-}$ to $Mo^{IV}$ or possibly $Mo^{V}$ polysulfido anions and that some product of this reduction has strong affinity for pyrite surfaces. $Mo^{IV,V}$ polysulfido anions are well known in the laboratory (Draganjac et al., 1982; Pan et al., 1983; Harmer et al., 1986; Hadjikyriacou and Coucouvanis, 1987; Coucavanis et al., 1989), but their syntheses generally have involved geochemically inapplicable conditions (high Mo concentrations, organic counter ions, nonaqueous solvents, etc.).

This study was prompted by unexpected observations. During reaction of $MoOS_3^{2-}$ to form $MoS_4^{2-}$ in the presence of natural kaolinite, new dissolved Mo species, other than those in the $Mo^{VI}O_xS_{4-x}^{2-}$ series, appeared in solution; simultaneously the suspended solids scavenged a minor fraction (5–15%) of dissolved Mo (Vorlicek, 2002). From optical absorption spectra, it was clear that polysulfide ions were forming in the anoxic solutions, presumably because accessory ferric minerals in the kaolinite were oxidizing $HS^-$. The same kaolinite had not scavenged $MoS_4^{2-}$ and $MoOS_3^{2-}$ in previous experiments, which contained too little $\Sigma S^{2-}$ to produce significant amounts of polysulfides by reaction with accessory $Fe^{III}$ minerals (Vorlicek and Helz, 2002). These observations led to the hypothesis that polysulfide ions facilitate Mo scavenging.

* Author to whom correspondence should be addressed (gh17@umail.umd.edu).
†*Present address:*Department of Chemistry and Geology, Minnesota State University, Mankato, MN 56001, USA.

## 2. EXPERIMENTAL METHODS

### 2.1. Materials

The following reagents were purchased and used as received: $Na_2B_4O_7 \cdot 10H_2O$ (J.T. Baker), orthorhombic sulfur (Aldrich), and hexane (J.T. Baker). $Cs_2MoOS_3$ was synthesized as described in Erickson (1998), using a method modified after Harmer and Sykes (1980). $Na_2MoS_4 \cdot 3.5H_20$ was synthesized as described in Vorlicek and Helz (2002). Natural pyrite (MCB Reagents) was leached for 24 h in 0.1 mol/L HCl to remove oxide coatings, then filtered and washed with 0.01 mol/L EDTA, washed with 0.1 mol/L NaHS for 24 h, filtered and washed again with water, followed by methanol and finally dried. After this, the $FeS_2$ was stored in a $N_2$-filled glove box. The BET specific surface area of this pyrite was 0.576 $m^2/g$ (determined by Quantachrome Instruments, Boynton Beach FL).

All test solutions were prepared in deionized $H_2O$ and were deoxygenated by bubbling with $N_2$ for ~30 min. The $N_2$ was passed through a Ridox column (Fisher) to remove traces of $O_2$. Stock solutions of 0.01 mol/L $MoOS_3^{2-}$ or $MoS_4^{2-}$ were prepared by dissolving $Cs_2MoOS_3$ or $Na_2MoS_4 \cdot 3.5H_20$ in deoxygenated, deionized water and were standardized by UV-vis spectroscopy. Stock solutions of 1.0 mol/L $HS^-$ were prepared by bubbling $H_2S$ (Air Products) through a deoxygenated 1 mol/L NaOH solution for ~45 min. For Runs A–E, a polysulfide stock solution was prepared by adding 500 mL of 10 mM borate buffer (pH 8.2) to 1.0 g of elemental S and bringing the mixture to 1.0 mM NaHS with the 1.0 mol/L NaHS stock solution. This was stirred for 5 d in the glove box, during which excess solid S remained visibly present.

To prepare runs with different polysulfide/sulfide ratios, filtered (0.45 $\mu$m) aliquots of this polysulfide stock solution were mixed with aliquots of 1.0 mM NaHS, also containing 10 mM borate buffer at pH 8.2. Runs I-M made use of similar stock solutions containing 5.0 mM NaHS. For Runs F-H, a stock polysulfide solution was prepared by adding 25 mL of 1.0 mol/L NaHS to 0.8 g orthorhombic sulfur; the suspension was capped and allowed to age in an $N_2$-filled glove box. This solution contained $\Sigma S^{2-} = 0.94$ mol/L at pH 8.14; solid $S^0$ was visibly present. Runs F-H were prepared by dilution of the filtered stock solution. All solutions were pH-adjusted to 8.2 after mixing. Runs N and O involved a stock solution containing 3.0 mM $\Sigma S^{2-}$, 0.07 mol/L NaCl, 1 mM total Borate buffer. Run O additionally included 1.2 g/L solid S whereas Run N had no added S. The pH of both solutions was adjusted to 8.5 after addition of 0.35 mM$MoOS_3^{2-}$. Optical absorption spectra of final mixtures were used in combination with $\Sigma S^{2-}$, pH and ionic strength to calculate $\Sigma S^0$ and the concentrations of individual polysulfide ions (see section 2.3).

### 2.2. Experimental Procedures

Reactions between thiomolybdates and polysulfides were conducted at room temperature (23 ± 2°C) under $N_2$ in a glove box. At various times during reactions, aliquots of test solutions were filtered into plastic centrifuge tubes using 0.45 $\mu$m syringe filters (polysulfone membrane, Pall Gelman Laboratory). After measuring the pH of the samples and withdrawing an aliquot for $\Sigma S^{2-}$ analysis, the capped tubes were passed out of the glove box and UV-vis spectra were recorded. The samples were then frozen and saved for atomic absorption spectroscopy ($N_2O$-acetylene flame) to determine total Mo. Before AA, samples were pretreated with BrCl to oxidize sulfide. Aluminum (1000 ppm) was used as a matrix modifier.

Thiomolybdates were monitored using UV-vis spectroscopy vs. a deionized $H_2O$ blank. Depending on absorbance levels, 0.1 cm, 1 cm, or 10 cm quartz cuvettes were used. Extinction coefficients at 2 nm intervals between 276 and 500 nm are given by Erickson (1998) for all four thiomolybdates; additional extinction coefficients up to 700 nm for $MoS_4^{2-}$ are reported by Vorlicek (2002).

Total sulfide ($\Sigma S^{2-}$) in stock solutions was determined by titration. Test solutions were added to ~60 mL deoxygenated, deionized water, brought to pH 13 with NaOH and titrated with $HgCl_2$ using a Brinkmann Metrohm 716 DMS Titrino automatic titrator equipped with a $Ag/Ag_2S$ indicating electrode and a double junction reference electrode. The indicating electrode responds to decreasing free sulfide as HgS precipitates.

Attempts to identify Mo-polysulfido species by NMR were unsuccessful despite using test solutions containing 1 mM Mo, i.e., 2–5-fold greater than in the solutions used in most of this work. Twenty hour runs with a Bruker AV-400 MHz NMR equipped with a 10 mm broad band probe produced only weak signals ascribable to thiomolybdates. Experiments with and without locking on 10% $D_2O$ were performed.

Table 1. Initial concentrations in test solutions.[a]

| Run | pH | I (mM) | $\Sigma S^{2-}$ (mM) | $[HS^-]^b$ (mM) | $\Sigma S^{0b}$ (mM) | $[S_5^{2-}]^b$ (mM) | $[S_4^{2-}]^b$ (mM) | $[S_8]$ (aq)[b] (nM) |
|---|---|---|---|---|---|---|---|---|
| A | 8.2 | 2.0 | 1.08 | 1.00 | 0.05 | 0.004 | 0.01 | 0.13 |
| B | 8.2 | 2.2 | 1.16 | 1.02 | 0.273 | 0.032 | 0.048 | 7.4 |
| C | 8.2 | 2.2 | 1.06 | 0.888 | 0.401 | 0.051 | 0.065 | 25 |
| D | 8.2 | 2.4 | 1.21 | 0.997 | 0.521 | 0.068 | 0.083 | 33 |
| E | 8.2 | 2.5 | 1.13 | 0.863 | 0.740 | 0.102 | 0.110 | 102 |
| F | 8.2 | 0.8 | 0.47 | 0.380 | 0.230 | 0.031 | 0.036 | 54 |
| G | 8.2 | 1.3 | 0.94 | 0.773 | 0.409 | 0.053 | 0.064 | 38 |
| H | 8.2 | 2.5 | 1.88 | 1.56 | 0.768 | 0.099 | 0.124 | 29 |
| I | 8.2 | 5.5 | 4.83 | 4.55 | 0.016 | 0.0008 | 0.0004 | <0.01 |
| J | 8.2 | 6.3 | 4.80 | 4.20 | 1.19 | 0.140 | 0.210 | 6.7 |
| K | 8.2 | 6.8 | 4.92 | 4.14 | 1.84 | 0.231 | 0.305 | 19 |
| L | 8.2 | 7.0 | 4.73 | 3.78 | 2.49 | 0.329 | 0.390 | 45 |
| M | 8.2 | 7.9 | 4.96 | 3.66 | 3.75 | 0.523 | 0.550 | 117 |
| N | 8.5 | 74 | 3.00 | 2.74 | 0.636 | 0.059 | 0.132 | 0.3 |
| O | 8.5 | 74 | 3.00 | 2.46 | 1.59 | 0.177 | 0.291 | 3.3 |

[a] Initial Mo composition: runs A–H, 0.040 mM $MoOS_3^{2-}$; runs I—M, 0.040 mM $MoS_4^{2-}$; runs O and P, 0.35 mM $MoOS_3^{2-}$ and 0.07 M NaCl.
[b] Values calculated (see section 2.3).

### 2.3. Sulfur Speciation Calculations

In addition to reporting measured initial values of pH and $\Sigma S^{2-}$, Table 1 presents initial values of $HS^-$, $\Sigma S^0$, the two principal polysulfide ions ($S_5^{2-}$, $S_4^{2-}$) and $S_8$(aq). The latter five values were derived as follows from optical absorption spectra covering the 300–500 nm range.

The total dissolved sulfide in a solution after equilibration with elemental sulfur but before addition of any Mo compound can be represented as follows:

$$\sum S^{2-} = [H_2S] + [HS^-] + [S_5^{2-}] + [S_4^{2-}] \ldots \quad (1)$$

Brackets designate molar concentrations. Additional polysulfide ions, including protonated forms, were included in this equation in our calculations but only $S_5^{2-}$ and $S_4^{2-}$ were significant. By introducing the first ionization constant for $H_2S$ ($K_{H2S}$) and equilibrium constants for reactions of the type,

$$(n-1)\,S(s) + HS^- \leftrightarrow S_n^{2-} + H^+ \quad K_n = \frac{[S_n^{2-}]\,\gamma_2\,(10^{-pH})}{[HS^-]\,\gamma_1 a_s^{(n-1)}} \quad (2)$$

$$[HS^-]\,\gamma_1 = \frac{\sum S^{2-}}{\gamma_1^{-1} + \dfrac{10^{-pH}}{K_{H2S}} + \dfrac{K_5(a_s)^4}{\gamma_2(10^{-pH})} + \dfrac{K_4(as)^3}{\gamma_2(10^{-pH})}} \ldots \quad (3)$$

Here, $\gamma_1$ and $\gamma_2$ are activity coefficients for singly and doubly charged ions (computed from the Davies equation) and $a_S$ is the activity of zero-valent sulfur; a value of $a_S = 1$ characterizes a system saturated with solid rhombic sulfur. Values of $K_n$ were compiled by Shea and Helz (1988), based largely on Giggenbach (1974). The molecular solubility of sulfur is given by the following equation based on a constant by Boulegue (1978):

$$K_{S8} = 1.9 \times 10^{-8} = \frac{\gamma_0[S_8]}{a_S^{\,8}} \quad (4)$$

Because our experiments were performed at low ionic strength, $\gamma_0$ for uncharged species ($H_2S$, $S_8$) was set to unity.

Note that by linking the thermodynamic variable, $a_S$, to the molar concentration of $S_8$, Eqn. 4 sheds light on the physical meaning of $a_S$. Like the more familiar variable, pE, $a_S$ is a virtual quantity in the sense that its value corresponds to the concentration of no one compound. Instead, its value is linked to the concentrations of all $S^0$-bearing aqueous species by thermodynamic-based relationships (e.g., Eqn. 2 and 4). The scale for $a_S$ is such that $a_S = 1$ in a system in equilibrium with rhombic sulfur.

Absorption spectra were fit interatively: a trial value of $a_S$ was assumed and used to calculate a provisional value of [$HS^-$] using Eqn. 3. The trial value of $a_S$ and the provisional value of [$HS^-$] were then used to calculate provisional values of the polysulfides and $S_8$ using Eqn. 2 and 4. From these provisional values, a polysulfide absorption spectrum was calculated and compared to an observed spectrum.

$$\text{Absorbance} = \varepsilon_{S5}[S_5^{2-}] + \varepsilon_{S4}[S_4^{2-}] \ldots \quad (5)$$

Extinction coefficients ($\varepsilon$) for polysulfide species were calculated as a function of wavelength from gaussian functions (Giggenbach, 1972). Optical absorption by $S_8$ was neglected because its concentration was always small. Calculated and observed spectra were compared at every 2 nm between 300 and 500 nm. In subsequent iterations, $a_S$ was adjusted to minimize the squares of the deviations between the observed and calculated spectra. Once the optimum $a_S$ was obtained, final concentrations of all species containing $S^0$ could be calculated via Eqns. 2 and 4.

When this approach was used to estimate $a_S$ in solutions containing $MoOS_3^{2-}$ and $MoS_4^{2-}$, terms were added to Eqn. 5 for the absorption due to these Mo species, and the concentrations of $MoOS_3^{2-}$ and $MoS_4^{2-}$ were also adjusted to optimize the fit by the method of least squares.

As a test of the reproducibility of this approach, a polysulfide solution having a composition similar to that of Run G but containing no Mo was sampled five times over a 48 h period. The mean and standard deviation of the five $\Sigma S^0$ values calculated from the resulting spectra were 0.482 ± 0.008 mM. A sixth sample taken after 98 h gave a higher $\Sigma S^0$, probably because some oxidation of $HS^-$ had occurred. This test suggests that the reproducibility associated with measuring absorption spectra and deriving values for $\Sigma S^0$ is better than ±22%; reproducibility of $S_5^{2-}$ and $S_4^{2-}$, the principal components of $\Sigma S^0$, is comparable. Reproducibility of $S_8$ is ~10%.

In another test, we checked whether the calculated $\Sigma S^0$ concentrations were consistent with dilution factors used in preparing the solutions. Based on dilution factors, $\Sigma S^0$ for runs B to E and J to M should be in the ratios, 0.67:1:1.33:2. Calculated ratios in Table 1 are 0.68:1:1.30:1.85 for B to E and 0.65:1:1.35:2.04 for J to M. Agreement is thus reasonably good. It must be noted, however, that these tests do not account fully for systematic errors that might arise from errors in extinction coefficients, equilibrium constants or activity coefficients.

One intriguing feature of the calculated results in Table 1 is that [$S_8$] often exceeds saturation with respect to rhombic sulfur (19 nM; Eqn. 4). Runs E and M, which involve undiluted stock solutions that had been in contact with rhombic S for a week, appear to be 5- or 6-fold supersaturated with respect to solid $S_{rhom}$, as judged by the concentration of $S_8$. Supersaturation might have arisen either because of acidification associated with final pH adjustment after filtering off $S_{rhom}$ or because stock solutions had equilibrated with a metastable (e.g., colloidal) form of S rather than less-soluble, thermodynamically stable $S_{rhom}$. Natural waters near sharp redox gradients also appear to be considerably supersaturated with respect to $S_{rhom}$ when subjected to a thermodynamic speciation analysis similar to that used here (Wang et al., 1998). This demonstrates that equilibration of aqueous sulfide solutions with particulate S at near-neutral pH is slow.

## 3. RESULTS

### 3.1. Homogeneous Reactions of $MoOS_3^{2-}$ and $MoS_4^{2-}$ in Polysulfide Solutions

The upper panel of Figure 1 shows spectral changes occurring during reaction of $MoOS_3^{2-}$ with $HS^-$ in the presence of polysulfides. Initial sulfide is large enough that most of the

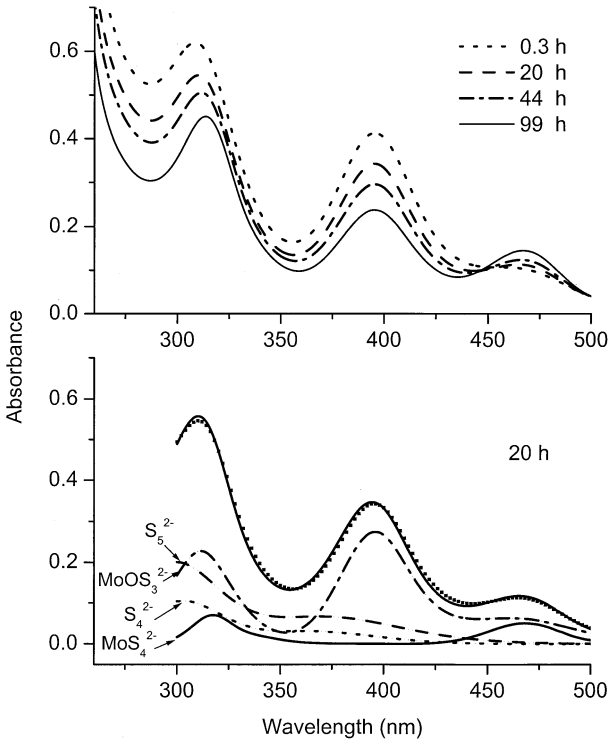


Fig. 1. (top) Changes in optical absorption observed in a 1 cm cell during the course of Run F (see Table 1 for solution composition). (bottom) Illustration of a fit to one of the spectra in the upper figure; small squares represent observed absorbances at 2 nm intervals and the heavy curve through the squares shows the fitted total absorbance. Lighter weight lines near the bottom of the lower panel show fit-generated individual absorbances of the four dissolved chromophores that contribute most of the total absorbance. According to the fit, the solution in the lower panel contains 30 $\mu$M $MoOS_3^{2-}$ and 4 $\mu$M $MoS_4^{2-}$. Because $\Sigma$Mo is 40 $\mu$M in this experiment, 6 $\mu$M Mo is unaccounted for at this time in the experiment. The fraction unaccounted for, $\Sigma Mo_{Deficit}$, grows to 13 $\mu$M by 99 h.

$MoOS_3^{2-}$ is expected on thermodynamic grounds to transform to $MoS_4^{2-}$. The lower panel of Figure 1 gives a representative example of a fit to one spectrum (20 h) in the upper panel. Concentrations derived from this fit are given in the caption.

Spectral changes with time in Figure 1 differ from those found when polysulfides are negligible. Without polysulfides, $MoS_4^{2-}$ peaks centered at 318 and 468 nm grow as the $MoOS_3^{2-}$ peak centered at 396 nm falls (Harmer and Sykes, 1980; Brule et al., 1988; Erickson and Helz, 2000). Because the molar extinction coefficient for the 468 nm $MoS_4^{2-}$ peak (11870) is larger than that for the 396 nm $MoOS_3^{2-}$ peak (9030), the rising $MoS_4^{2-}$ peak would become larger than the falling $MoOS_3^{2-}$ peak if stoichiometric replacement of $MoOS_3^{2-}$ by $MoS_4^{2-}$ were occurring. This behavior clearly is not observed in the upper panel of Figure 1. Instead, loss of $MoOS_3^{2-}$ is accompanied by much less $MoS_4^{2-}$ production, observable only at 468 nm. By the end of the experiment (99 h), ~20 $\mu$M $MoOS_3^{2-}$ has disappeared, but less than 8 $\mu$M $MoS_4^{2-}$ has appeared. In the vicinity of the 318 nm $MoS_4^{2-}$ peak, absorbance declines, rather than rises, as $MoOS_3^{2-}$ disappears. The general decline in absorbance at all wavelengths

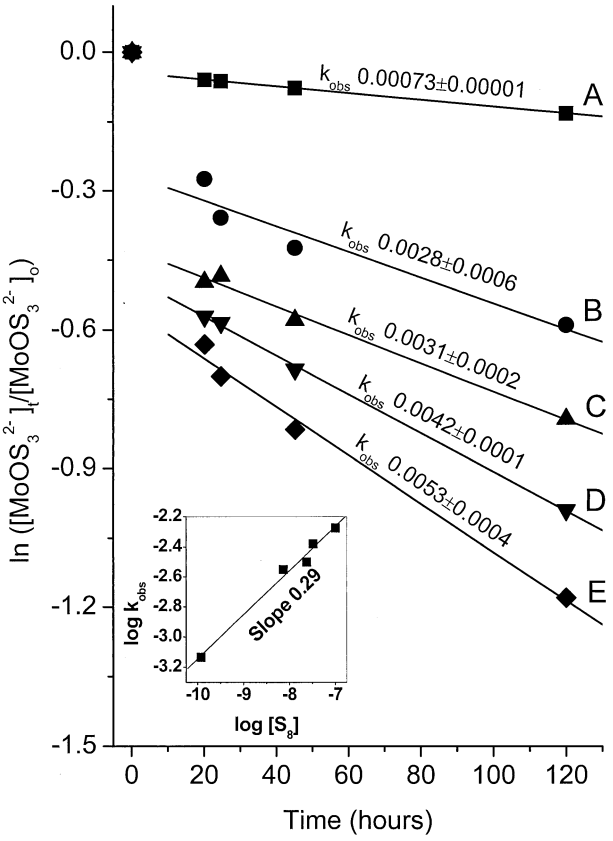


Fig. 2. Decay of $MoOS_3^{2-}$ in Runs A to E, which have similar $\Sigma S^{2-}$; faster decay rates are associated with higher initial dissolved $\Sigma S^0$ (see Table 1 for initial concentrations). Observed rate constants, $k_{obs}$ ($h^{-1}$), are equal to the slopes of the lines in this plot; uncertainties are standard deviations of the slopes. The inset shows that $k_{obs}$ values correlate with initial $S_8$ concentration.

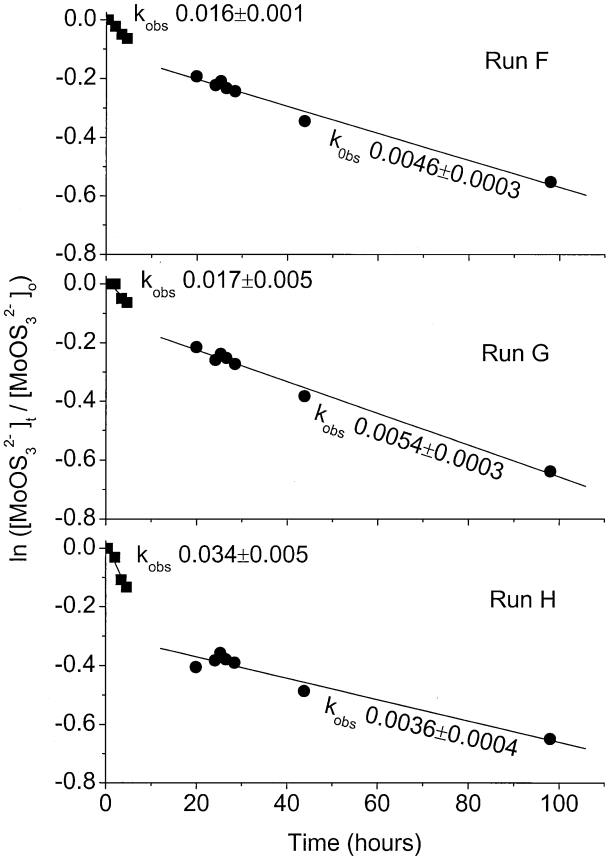


Fig. 3. Pseudo-first-order plots of the $MoOS_3^{2-}$ loss in experiments having similar $[S_8]$ but differing $\Sigma S^{2-}$.

below ~450 nm can be attributed to loss of dissolved polysulfides.

The Mo deficit that has accumulated over the course of the experiment cannot be attributed to precipitation of Mo; atomic absorption analyses show that total dissolved Mo changes by <5%. The pattern in Figure 1 is consistent with a reaction between $MoOS_3^{2-}$ and polysulfides, producing one or more spectrally invisible products in addition to $MoS_4^{2-}$.

Figure 2 shows the loss of $MoOS_3^{2-}$ over time in a series of experiments in which pH and $\Sigma S^{2-}$ are approximately constant but $\Sigma S^0$ is varied. Again, $MoS_4^{2-}$ is favored thermodynamically relative to $MoOS_3^{2-}$ in all runs. Concentrations of $MoOS_3^{2-}$ were calculated from spectra like those in Figure 1. Approximate linearity of the data in Figure 2 implies that $MoOS_3^{2-}$ is decomposing by a first order process; slopes of the regression lines give values for $k_{obs}$. However, decay of $MoOS_3^{2-}$ during the first 24 h is faster than subsequent decay, indicating that the process is more complex than a single-step, first order decay. In the absence of added $S^0$ (Run A), loss of $MoOS_3^{2-}$ is very small over 120 h or 5 d (consistent with expectations from prior experience; Erickson and Helz, 2000).

Runs A–E demonstrate that increasing the initial $S^0$ concentration increases the rate of loss of $MoOS_3^{2-}$. In the inset to Figure 2, log $k_{obs}$ obtained from the regression lines, has been plotted as a function of the log of the initial $S_8$ concentration (Table 1). An excellent correlation with a slope of 0.29 is obtained. (Note that $S_8$ does not change greatly during runs B-E, despite its very low initial concentration, because it is buffered by $S_5^{2-}/S_4^{2-}$; total $S^0$ contained in these anions is large relative to the amount of Mo reacting.) Production of $MoS_4^{2-}$ during these experiments was far smaller than the $MoOS_3^{2-}$ loss and was scarcely quantifiable (mostly < 0.002 mM and always <0.004 mM); $MoOS_3^{2-}$ is decaying primarily to optically invisible products. No loss in dissolved ΣMo was detected by atomic absorption in any of these experiments.

Figure 3 shows $MoOS_3^{2-}$ loss for three test solutions containing varying $\Sigma S^{2-}$ and $\Sigma S^0$, but having similar $\Sigma S^{2-}/\Sigma S^0$ ratios. By breaking the data into segments taken before and after 20 h, this figure highlights the change in the rate of $MoOS_3^{2-}$loss early in the these experiments. Note that the rate of $MoOS_3^{2-}$ loss in the 20–100 h time window is similar in all runs and similar to rates in Figure 2. Significantly, the rate of loss does not correlate with initial $[HS^-]$, $[S_5^{2-}]$ or $[S_4^{2-}]$, which vary by 3- to 6-fold (Table 1).

In an effort to explore the characteristics of the optically invisible intermediate components, we used hexane to extract $S^0$ from a solution like that in run F after 30 h reaction time. As shown in Figure 4, lowering the $\Sigma S^0$ in this manner did not cause reversal of the $MoOS_3^{2-}$ loss, but instead caused rapid

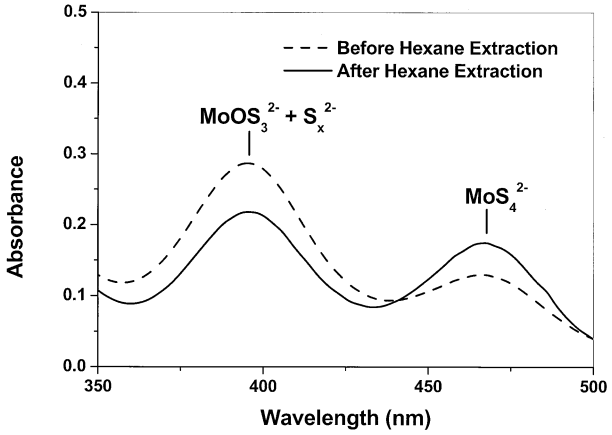


Fig. 4. Effect of hexane extraction on the absorption spectrum from a solution like that in Run F after 30 h reaction time (1 cm absorption cell; $V_{hexane}/V_{aqueous} = 1$). After extraction, the hexane contained 0.021 mM $S^0$. Calculated $\Sigma Mo_{Deficit}$ was little changed before and after extraction (8.1 ± 9.1 $\mu$M), while $MoOS_3^{2-}$ dropped (25.4 → 19.6 $\mu$M) and $MoS_4^{2-}$ rose (6.5 → 11.3).

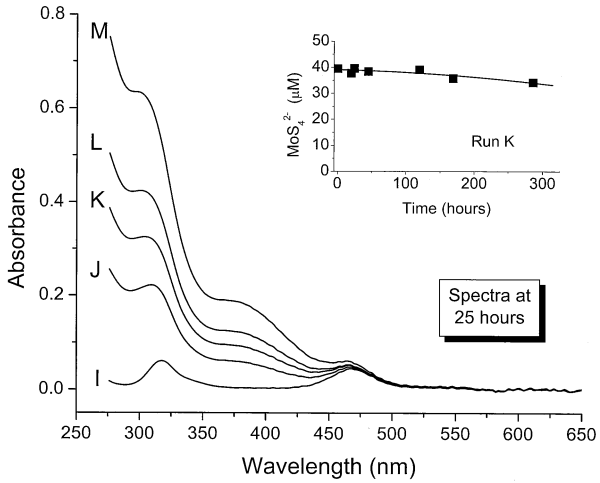


Fig. 5. Evidence of little or no reaction between $MoS_4^{2-}$ and polysulfides (Runs I-M). Spectra taken after 25 h = reaction (1 cm cell). $\Sigma S^0$ increases from Run I to M. These spectra differ chiefly in the amount of polysulfide present. In all runs, the calculated concentration of $MoS_4^{2-}$ changes very little in the first 100 h (one example shown in inset). At longer times, $MoS_4^{2-}$ is lost slowly.

doubling of the $MoS_4^{2-}$ concentration (as well as loss of polysulfide absorbance). Fits of the two spectra suggest that most of the new $MoS_4^{2-}$ formed at the expense of $MoOS_3^{2-}$. The dissolved Mo that was unaccounted for optically ($\Sigma Mo_{Deficit}$) remained nearly constant. Apparently the components of $\Sigma Mo_{Deficit}$ are not labile on a time scale of minutes. Because conversion of $MoOS_3^{2-}$ to $MoS_4^{2-}$ is slow in the absence of hexane, rapid conversion in this experiment suggests that a nonpolar, hexane-soluble intermediate exists. Such an intermediate might be related to known solids like $MoS_{3+n}$, n = 0–3; these always-amorphous solids are thought to be composed of oligomers (Hibble et al., 2001; Afanasiev and Bezverkhy, 2002). It is plausible that such oligomers would form in hexane and serve as reaction intermediates even when the accompanying aqueous phase is undersaturated with respect to a $MoS_{3+n}$ phase.

Figure 5 shows results of experiments to determine if $MoS_4^{2-}$ reacts with polysulfides. Coyle et al. (1992) studied analogous reactions between $MoS_4^{2-}$ and organic disulfides in dimethylformamide. Over ~15 min, they observed substantial loss of $MoS_4^{2-}$ and formation of green monomers ($\lambda_{max}$ 620 nm) which in turn transformed during a few hours to $Mo_2S_8^{2-}$ dimers ($\lambda_{max}$ 572 nm). In contrast, Figure 5 shows that no peaks appear in the 550–650 nm region when $MoS_4^{2-}$ is exposed even for hours to polysulfides in aqueous solution. Analyses of our spectra indicate presence only of $MoS_4^{2-}$ and polysulfides during a contact time of up to 300 h.

The inset to Figure 5 presents evidence for a small amount of $MoS_4^{2-}$ loss over the test period. This was observed in all five runs, but the amount of reaction was never large enough in relation to experimental uncertainty to permit a quantitative kinetic analysis. The degree of reaction appeared not to correlate with initial concentrations of dissolved S species and may have been controlled by extraneous factors such as oxidation, which even inside a glove box is difficult to eliminate in long experiments.

### 3.2. Scavenging of Thiomolybdates by Pyrite Surfaces

The effect of $S^0$ on the tendency of aqueous Mo to attach to pyrite was explored in two experiments in which $MoOS_3^{2-}$ was allowed to react with polysulfides in experiments similar to those shown in Figures 2 and 3. The two solutions contained 0.35 mM $MoOS_3^{2-}$, 3.0 mM $\Sigma S^{2-}$, 1.0 mM borate buffer and 70 mM NaCl. One solution, Run O, also received 1.2 g/L of powdered sulfur. Periodically, 5 mL aliquots of these solutions were filtered (0.45 $\mu$m) into plastic centrifuge tubes containing 0.100 g pyrite, which had been prepared as described in Section 2.1. The resulting slurries contained 20 g/L pyrite (surface concentration, 11.5 $m^2$/L). The solutions were shaken by hand for 10 min and then filtered and removed from the glove box. Optical absorption spectra of the filtered aliquots were compared with similar 5 mL aliquots that had not been exposed to pyrite. Subsequently, atomic absorption analyses were done to determine $\Sigma Mo$.

Figure 6 shows the evolution of the Mo species during these experiments. Run N, containing less $\Sigma S^0$ than Run O, slowly produces a pool of optically invisible intermediates, represented by $\Sigma Mo_{Deficit}$. In Run O, a pool of intermediates forms rapidly and appears to reach a steady state concentration. Decay of $MoOS_3^{2-}$ and formation of $MoS_4^{2-}$ are faster than in Run N.

In both runs, AA-determined $\Sigma Mo$ does not change within analytical uncertainty during a period of 965 h (40 d). Despite $\Sigma Mo$ concentrations 1000-fold higher than in seawater, no precipitation occurs in either experiment. This result is even more striking if the degree of saturation with respect to molybdenite, $MoS_2$, is considered. From thermodynamic tables (Wagman et al., 1982), an equilibrium constant can be computed for $MoO_4^{2-}$ in equilibrium with $MoS_2$. Combining this with a constant for equilibrium between $MoO_4^{2-}$ and $MoOS_3^{2-}$ from Erickson and Helz (2000) yields log K = −29.63 for $MoS_2(s)+S(s)+H_2O(l) = 2H^+ + MoOS_3^{2}$. Accord-

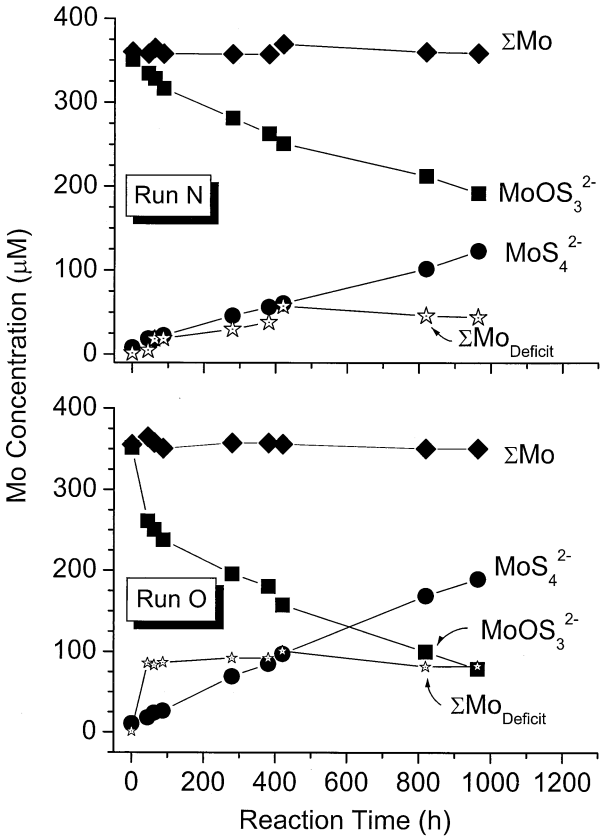


Fig. 6. Time-evolution of the solutions used in the pyrite-scavenging experiments. Run N: Low $S^0$. Run O: High $S^0$ (see Table 1 for solution compositions). $Mo_{Total}$ determined by atomic absorption; $MoOS_3^{2-}$ and $MoS_4^{2-}$ determined by optical absorption; $\Sigma Mo_{Deficit}$ determined by difference between ΣMo and the sum of the two thiomolybdates. The rate of $MoS_4^{2-}$ production is ~10-fold greater in Run O than would occur in a solution containing no $S^0$ (the latter rate estimated from Erickson and Helz, 2000).

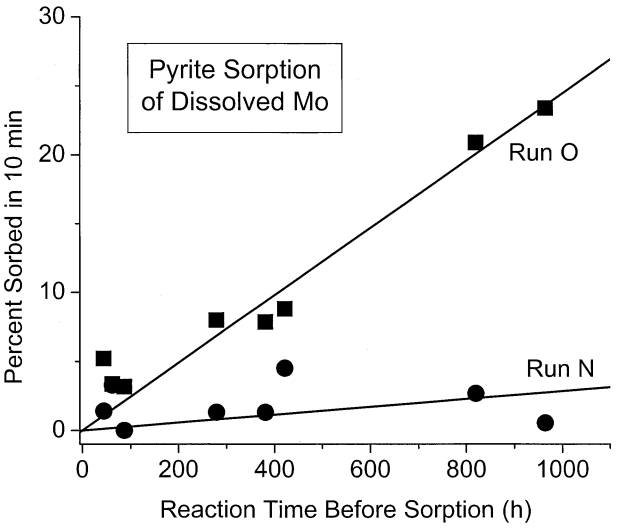


Fig. 7. Percent of dissolved Mo scavenged by pyrite in 10 min plotted vs. the time of $MoOS_3^{2-}$ decay before introduction of the pyrite. Run N: Low $S^0$. Run O: High $S^0$ (see Table 1 for solution compositions). Evolution of the dissolved Mo species distribution for these runs is shown in Figure 6.

ing to this value of K, Run O initially was supersatured with respect to $MoS_2$ by $>10^9$.

Figure 7 shows the percentage of ΣMo that can be scavenged by pyrite from the solutions in Figure 6. After 965 h, approximately 80 μM ΣMo in Run O has been transformed to one or more chemical species that sorb quickly to $FeS_2$. The maximum surface concentration is $7 \times 10^{-6}$ moles/$m^2$ or ~4 Mo atoms/$nm^2$, a high degree of coverage. These experiments differ from those of Bostick et al. (2003) in that the contact time with the pyrite surface was kept very brief to minimize the effect of the surface on dissolved Mo species.

Early in both Run N and O, scavengable Mo appears to be negligible (experimental uncertainty is large because the plotted points represent small differences between much larger numbers). Negligible scavenging implies that neither $MoOS_3^{2-}$ nor the early-formed components of $\Sigma Mo_{Deficit}$ in Run O strongly sorb to pyrite. Over a reaction period of 965 h, ~0.08 mM of ΣMo becomes scavengable in $S^0$-saturated Run O but <0.01 mM becomes scavengable in Run N. Because similar amounts of $MoS_4^{2-}$ are produced in both runs but a scavengable form of Mo is produced mainly in Run O, it further appears that $MoS_4^{2-}$ is not the form of dissolved Mo sorbed to pyrite. Instead, the scavengable form of Mo appears to be one of the optically invisible components formed slowly in the $\Sigma Mo_{Deficit}$ pool. Under limited $\Sigma S^0$ conditions (Run N), very little Mo is converted to a scavengable form, but under $S^0$-saturated conditions (Run O) a scavengable species gradually appears.

## 4. DISCUSSION

### 4.1. Ligand-Induced Reduction

Polysulfide ligands bound to dissolved $Mo^{VI}$ species are known to promote reduction, forming $Mo^{IV}$ and $Mo^{V}$ species. This phenomenon, ligand-induced reduction, was first discovered in the case of Mo about two decades ago (Müller et al., 1978; Draganjac, et al., 1982; Pan et al., 1983). The phenomenon has been recognized also in the chemistry of $V^V$, $W^{VI}$ and $Re^{VII}$ (Cohen and Stiefel, 1985; Halbert et al., 1986; Müller et al., 1991; Murray et al., 1995; McConnachie and Stiefel, 1999). Conceivably, it plays an as yet unexplored role in the geochemistry of a number of thioanion-forming, redox sensitive trace elements.

In ligand-induced reduction of $Mo^{VI}$, a $S^0$-donating reactant in net effect converts a pair of $S^{2-}$ ligands in a thiomolybdate ion to a bidentate $S_n^{2-}$ ligand (Harmer et al., 1986; Coucouvanis, 1998). The $S^0$-donating reactant may be a polysulfide ion, an $S_8$ molecule or an organic di- or polysulfide. In this process, an electron pair is transferred from one $S^{2-}$ ligand to the $Mo^{VI}$ center, reducing it to $Mo^{IV}$. Subsequently, the new $Mo^{IV}$ species often combines with another $Mo^{VI}$ thiomolybdate to form a $Mo^{V}_2$ dimer, which is stabilized by Mo-Mo bonding. Ligand-induced reduction has been described as seemingly paradoxical (Harmer et al., 1986) because reduction of the $Mo^{VI}$ center is induced by an oxidizing agent ($S^0$ donor), rather than by a reducing agent.

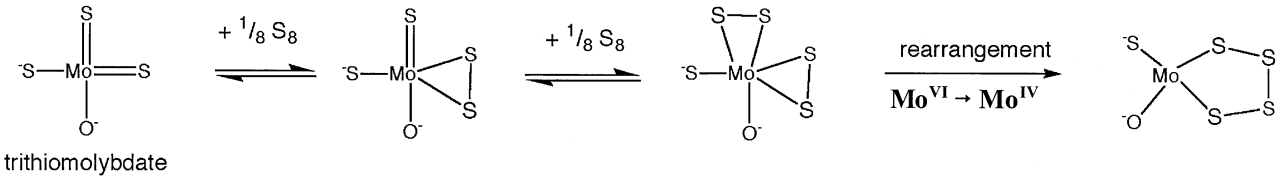


Fig. 8. Reaction scheme to explain the rate of $MoOS_3^{2-}$ loss in Figures 2, 3 and 6.

Known products of the reactions of $S^0$-donors with thiomolybdates are numerous but many can be classified into monomeric ($Mo^{IV}$) and dimeric ($Mo^{V}_2$) series:

$$MoOS_3^{2-} + n/8\,S_8(aq) \rightarrow Mo^{IV}OS_{3+n}^{2-} \quad (6)$$

$$MoS_4^{2-} + n/8\,S_8\,(aq) \rightarrow Mo^{IV}S_{4+n}^{2-}$$

$$2MoOS_3^{2-} + n/8\,S_8(aq) + H^+ \rightarrow Mo^{V}_2O_2S_{5+n}^{2-} + HS^- \quad (7)$$

$$2MoS_4^{2-} + n/8\,S_8(aq) + H^+ \rightarrow Mo^{V}_2S_{7+n}^{2-} + HS^-$$

Larger oligomers also are known but will not be discussed here. Well-known examples of monomers include $Mo^{IV}O(S_4)_2^{2-}$ and $Mo^{IV}S(S_4)_2^{2-}$. In these monomers, 5-coordinated Mo is bonded to two bidentate $S_4^{2-}$ ligands and a third = O or = S ligand. Well-known examples of dimers include $Mo^{V}_2O_2S_2(S_2)_2^{2-}$ and $Mo^{V}_2S_4(S_2)_2^{2-}$. Here, each Mo atom is coordinated by one bidentate disulfide ligand, one = O or = S ligand and is bridged via two $S^{2-}$ ligands to the other Mo atom, producing a symmetrical dimer. With addition of more $S^0$ to this series of dimers, the disulfide ligands expand to larger, bidentate polysulfide ligands. See Coucouvanis (1998) for a review of this chemistry.

Dimers are less likely to form in dilute solutions, and it remains to be seen if $Mo^{V}_2$ dimers are significant at Mo concentrations found in nature. Several known dimers have optical extinction coefficients $>10^4$ (Draganjac et al., 1982; Hadjikyriacou and Coucouvanis, 1987); these would have been detected if they had formed in our experiments.

### 4.2. Chemical Interpretation of Results

The $MoOS_3^{2-}$ behavior that we observe in the presence of polysulfides (Figs. 1–3 and 6) is consistent with ligand-induced reduction. Our inferred mechanism (see below) is portrayed in Figure 8.

Figure 3 indicates that the initial consumption rate of $Mo^{VI}OS_3^{2-}$ is directly proportional to polysulfide ion concentrations. A reaction that would explain this behavior is:

$$Mo^{VI}OS_3^{2-} + S_5^{2-} \rightarrow Mo^{VI}O(S_2)S_2^{2-} + S_4^{2-} \quad (8)$$

Because the rate of $Mo^{VI}OS_3^{2-}$ loss slows markedly during the first 20 h (Figs. 2 and 3), reaction 8 must become curtailed by its reverse reaction:

$$Mo^{VI}O(S_2)S_2^{2-} + S_4^{2-} \rightarrow Mo^{VI}OS_3^{2-} + S_5^{2-} \quad (9)$$

As these reactions come into equilibrium, further loss of $MoOS_3^{2-}$ becomes limited by consumption of the new product.

After 20 h, the rate of the latter process is proportional to $(S_8)^{\sim 0.29}$, as implied by the inset to Figure 2. It is significant that this rate is proportional to $[S_8]$ and not to concentrations of polysulfide ions. One way of explaining these facts is to propose that once the first product, $Mo^{VI}O(S_2)S_2^{2-}$, has formed a second $S^0$ atom is added rapidly:

$$Mo^{VI}O(S_2)S_2^{2-} + S_5^{2-} \leftrightarrow Mo^{VI}O(S_2)(S_2)S^{2-} + S_4^{2-} \quad (10)$$

After ~20 h, the second product will also have approached equilibrium with $MoOS_3^{2-}$ according to the net reaction:

$$Mo^{VI}OS_3^{2-} + 2S_5^{2-} \leftrightarrow Mo^{VI}O(S_2)(S_2)S^{2-} + 2S_4^{2-} \quad (11)$$

Because $S_5^{2-}$ and $S_4^{2-}$ are themsleves in equilibrium with $S_8$ and buffer it,

$$S_5^{2-} \leftrightarrow S_4^{2-} + 1/8\,S_8 \quad K_{12} = 0.14 \quad (12)$$

reaction 11 can be reformulated as the following equilibrium:

$$Mo^{VI}OS_3^{2-} + \frac{2}{8}S_8 \leftrightarrow Mo^{VI}O(S_2)(S_2)S^{2-}, \quad K_{13} = K_{11}/K_{12}^2 \quad (13)$$

We posit that the rate-controlling step after 20 h involves the ligand-induced reduction step:

$$Mo^{VI}O(S_2)(S_2)S^{2-} \rightarrow Mo^{IV}O(S_4)S^{2-} \quad (14)$$

Writing the rate law for this elementary reaction and employing the mass action law for Eqn. 13:

$$\text{Rate} = -k_{14}[Mo^{VI}O(S_2)(S_2)S^{2-}] = -k_{14}K_{13}[MoOS_3^{2-}][S_8]^{2/8} \quad (15)$$

Eqn. 15 rationalizes why, beyond 20 h, the observed rate of $MoOS_3^{2-}$ loss is 1st order in $MoOS_3^{2-}$, ~0.29th order in $S_8$ and independent of the concentrations of individual polysulfide ions, even though polysulfides are the main carriers of $S^0$ in solution. The reaction scheme on which Eqn. 15 is based (see Fig. 8) is concordant with similar proposals in the literature (Coucouvanis et al., 1989; Coyle et al., 1992; Coucouvanis, 1998). From observed rate constants in Figures 2 and 3, $k_{14}K_{13}$ is estimated to be $0.30 \pm 0.04$ mol/$L^{-0.25}h^{-1}$ (based on the assumption that $[S_8]$ is constant during the course of the reaction owing to the large excess of $\Sigma S^0$ relative to $\Sigma Mo$). The value of $K_{13}$ is estimated to be $10^{1.5 \pm 0.3}$.

Subsequently, the $Mo^{IV}$ product in reaction 14 might be subject to nucleophilic substitution by a second polysulfide ligand, replacing the O or the S ligand, and/or it might react

with $MoOS_3^{2-}$ to produce a $Mo^V$ dimer. Because these steps lie beyond the rate controlling steps for $MoOS_3^{2-}$ loss and produce no optical signals, our evidence reveals little about them. However, the evidence in Figures 6 and 7 indicates that further reactions indeed occur on a time scale >100 h. One leads to $MoS_4^{2-}$, which is only a minor product in the first 100 h. Another leads to a product that is quickly scavenged from solution by pyrite surfaces (Fig. 7).

Gradual appearance of $MoS_4^{2-}$ over the longer time period covered in Runs N and O (Fig. 6) implies that the polysulfido products formed from $MoOS_3^{2-}$ are unstable intermediates under the conditions of our experiments. Negligible reaction between polysulfides and $MoS_4^{2-}$, shown in Figure 5, supports this interpretation. Thus $MoS_4^{2-}$ appears to be the thermodynamically stable product when $[H_2S]$ is high enough to destabilize $MoO_4^{2-}$ (i.e., above the action point of the geochemical switch as described by Erickson and Helz, 2000). Note that decomposition of Mo polysulfido complexes to $MoS_4^{2-}$ must involve reversion of the oxidation state of Mo to +VI.

The ultimate stability of $MoS_4^{2-}$ in our experiments is not necessarily in conflict with evidence for ligand-induced reduction of $MoS_4^{2-}$ in dimethylformamide solvent (Coyle et al., 1992) or in aqueous solvent in the presence of a high concentration of $(NH_4)_2S_3$ (Draganjac et al., 1982). In both these cases, $MoS_4^{2-}$ may have become unstable with respect to polysulfido complexes because of the high concentrations of $S_8$ achievable in organic solvents or metastably in short-duration experiments in water. Over longer durations, precipitation of colloidal $S^0$ limits $[S_8]$ in aqueous solution to ~125 nM (LaMer and Dinegar, 1950). In run M (Fig. 5), $[S_8]$ was near this upper limit but $MoS_4^{2-}$ was nonetheless negligibly consumed.

$S^0$-mediated reduction probably occurs only after $MoO_4^{2-}$ in sulfidic water has been sulfidized as far as $MoOS_3^{2-}$. According to Harmer et al. (1986) reduction of thiomolybdates, $MoO_xS_{4-x}^{2-}$, becomes easier as the degree of sulfidation increases (i.e., x becomes smaller). They report that an organic disulfide reacts with $MoO_2S_2^{2-}$ to produce a $Mo^{VI}$ anion containing a disulfide ligand rather than a $Mo^{IV}$ or $Mo^V$ species.

### 4.3. Geochemical Implications of Results

The key finding from this work is that Mo speciation in sulfidic natural waters will be controlled not only by the activity of $H_2S$, as we have proposed in previous papers, but also by the activity of zero-valent sulfur. Few determinations of $[S_8]$ in anoxic natural waters are available, but they suggest that the concentrations employed in our experiments are representative of those in nature. For example, Wang et al. (1998) describe pore waters from lake sediments that contain the equivalent of 25–100 nM $[S_8]$ (compare with values in Table 1). These solutions were all supersaturated with respect to rhombic S, but probably undersaturated with respect to colloidal S. Polysulfides often exceed micromolar concentrations in sulfidic saltwaters (Boulegue et al., 1982; Luther et al., 1985; Shea and MacCrehan, 1988).

Our results suggest a model for how marine $MoO_4^{2-}$ might come to be fixed in Mo-Fe-S cuboidal structures associated with pyrite in anoxic sediments and black shales. The reaction pathway would involve stepwise conversion of $MoO_4^{2-}$ to $MoO_3S^{2-}$, $MoO_2S_2^{2-}$ and $MoOS_3^{2-}$ in the presence of $>10^{-5}$ M biogenic $H_2S$ (see Erickson and Helz, 2000). In the absence of $S^0$-donors, sulfide would eventually also replace the final O ligand, producing $MoS_4^{2-}$, but this last nucleophilic substitution could take decades to reach completion at seawater pH and temperature without mineral-surface catalysts. In the presence of $S^0$-donors, a faster homogeneous reaction pathway to thermodynamically stable $MoS_4^{2-}$ is available through Mo polysulfido intermediates. Spontaneously, Mo reduction occurs in these intermediates, lowering the coulombic resistance to forming cuboidal structures on pyrite. Coulombic resistance arises from short intercation distances in cuboidal structures (Bostick et al., 2003). Thus, as appropriate polysulfido species form, they can be scavenged by pyrite, diverting Mo from the stable, soluble product, $MoS_4^{2-}$. Existence of cuboidal Mo-Fe-S in Paleozoic black shales implies that these structures are extremely stable, once formed (Helz et al., 1996).

No critical redox potential or threshold that could control Mo fixation exists in the proposed reaction pathway (so long as redox conditions are appropriate for biologic sulfate reduction). The data in Figure 2 show that $MoOS_3^{2-}$ is consumed on geochemically rapid time scales over a broad $S_8$ concentration range, i.e., 1–2 orders of magnitude. A broad $S_8$ concentration range implies flexibility with respect to Eh, which tends to be controlled by the $\Sigma S^0/\Sigma S^{2-}$ ratio at a given pH in sulfidic waters (Boulegue and Michard, 1979).

It is possible that other reaction pathways exist for producing Mo-Fe-S cuboidal structures associated with pyrite. Nonetheless, we note two attractive features of the pathway proposed here. First, optimal conditions for ligand-induced reduction of Mo and for pyrite growth (Benning et al., 2000) are similar: both are favored in polysulfide-rich sulfidic waters. Second, the polysulfido ligand in a species such as $Mo^{IV}O(S_4)S^{2-}$ is expected to be labile to insertion of $S^0$ from donors that might include disulfide groups on pyrite surfaces. It is easy to imagine that an $Mo^{IV}O(S_4)S^{2-}$ ion could become doubly tethered by covalent linkages to pyrite when two adjacent disulfides on the mineral surface insert into and break open the polysulfide ring. Tethering would facilitate formation of cuboidal structures.

More remains to be learned about mineral surface processes leading to Mo fixation. Classic work (Sugawara et al., 1961; Bertine, 1972) showed that FeS precipitates scavenge Mo. Vorlicek (2002) extended these observations, demonstrating that many freshly precipitated metal sulfides indiscriminantly sorb $MoO_xS_{4-x}^{2-}$ species. Slightly sulfidized $MoO_4^{2-}$ (possibly mostly $MoO_3S^{2-}$) as well as fully sulfidized $MoS_4^{2-}$ are scavenged by FeS, CoS, ZnS, HgS and PbS precipitates to a significant degree; CuS scavenges $MoS_4^{2-}$ very effectively but scavenges sulfidized $MoO_4^{2-}$ weakly.

These processes may influence Mo concentrations ephemerally in sediment pore waters but probably do not explain Mo enrichments that are preserved over geologic time in black shales. Monosulfide precipitates, especially FeS, are not durable geologically. Sugawara et al. (1961) demonstrated that $O_2$ quickly recycles FeS-scavenged Mo to solution by oxidizing the substrate.

Pyrite is the principal sulfide mineral preserved in sedimentary rocks. Pyrite is known to capture Mo during diagensis (Huerta-Diaz and Morse, 1992; Dellwig et al., 2002; Müller,

2002) and to retain it in sedimentary rocks (Raiswell and Plant, 1980; Coveney, 1987). Bostick et al. (2003) show that pyrite sorbs both $MoO_4^{2-}$ and $MoS_4^{2-}$ effectively. The sorbed $MoO_4^{2-}$ occurs at least partly as an outer-sphere complex that is readily displaced by $OH^-$ and that gives an X-ray absorption spectrum nearly identical to $MoO_4^{2-}$. They point out that this kind of sorption also is unlikely to produce geologically robust Mo fixation. On the other hand at pH<6, they observed that $MoS_4^{2-}$ reacts irreversibly with pyrite. The bound product no longer gives an X-ray absorption spectrum of $MoS_4^{2-}$, but instead resembles that of a Mo-Fe-S cuboidal structure. Why such strongly bound Mo forms rapidly at pH <6 but very slowly at pH 8.5 in our experiments remains an open question. Possibly ligand-induced reduction occurs as a heterogeneous process directly on pyrite surfaces owing to $S^0$ normally found there (Nesbitt and Muir, 1994). Understanding mechanistically the interactions of dissolved Mo species with sulfide mineral surfaces is a rich field for future exploration.

*Acknowledgments*—This work was supported by NSF grant EAR 9980532 and EAR 0229387. MDK acknowledges support from a Carl Rollinson Undergraduate Research Fellowship, University of Maryland. Prof. Neil Blough contributed helpful suggestions. We thank Prof. John Morse and two anonymous reviewers for helpful suggestions.

*Associate editor:* M. Goldhaber

## REFERENCES

Adelson J. M., Helz G. R., and Miller C. V. (2001) Reconstructing the rise of recent coastal anoxia: Molybdenum in Chesapeake Bay sediments. *Geochim. Cosmochim. Acta* **65,** 237–252.

Afanasiev P. and Bezverkhy I. (2002) Synthesis of $MoS_x$ (5<x<6) amorphous sulfides and their use for preparation of $MoS_2$ monodispersed microspheres. *Chem Mater.* **14,** 2826–2830.

Benning L. G., Wilkin R. T., and Barnes H. L. (2000) Reaction pathways in the Fe-S system below 100°C. *Chem. Geol.* **167,** 25–51.

Bertine K. K. (1972) The deposition of molybdenum in anoxic waters. *Mar. Chem.* **1,** 43–53.

Bostick B. C., Fendorf S., and Helz G. R. (2003) Differential adsorption of molybdate and tetrathiomolybdate on pyrite ($FeS_2$). *Environ. Sci. Technol.* **37,** 285–291.

Boulegue J. (1978) Solubility of elemental sulfur in water at 298 K. *Phosphorus Sulfur* **5,** 127–128.

Boulegue J. and Michard G. (1979) Sulfur speciations and redox processes in reducing environments. *Chemical Modeling in Aqueous Systems* (ed. E. A. Jenne), pp. 25–50. Symposium Series 93. American Chemical Society.

Boulegue J., Lord C. J. III, and Church T. M. (1982) Sulfur speciation and associated trace metals (Fe, Cu) in the pore waters of Great Marsh, Delaware. *Geochim. Cosmochim. Acta* **46,** 453–464.

Brule J. E., Hayden Y. T., Callahan K. P., and Edwards J. O. (1988) Equilibrium and rate constants for mononuclear oxythiomolybdate interconversions. *Gaz. Chim. Ital.* **118,** 93–99.

Brumsack H. J. (1989) Geochemistry of recent TOC-rich sediments from the Gulf of California and the Black Sea. *Geol. Rundschau.* **78,** 851–882.

Cohen S. A. and Stiefel E. I. (1985) Dinuclear tungsten(V) and molybdenum(V) compounds containing $M_2S_2(\mu\text{-}S)_2^{2+}$ cores. Synthesis and reactivity of $[N(C_2H_5)_4]_2M_2S_{12}$ (M = W or Mo) and the crystal structure of $[N(C_2H_5)_4]_2W_2S_2(\mu\text{-}S)_2(S_4)_2$. *Inorg. Chem.* **24,** 4657–4662.

Coucouvanis D. (1998) Synthesis, structures, and reactions of binary and tertiary thiomolybdate complexes containing the (O)Mo($S_x$) and (S)Mo($S_x$) functional groups (x = 1,2,4). *Adv. Inorg. Chem.* **45,** 1–73.

Coucouvanis D., Toupadakis A., Koo S.-M., and Hadjikyriacou A. (1989) An inorganic functional group approach to the systematic synthesis and reactivity studies of binuclear Mo/S and Mo/S/O complexes. *Polyhedron* **8,** 1705–1716.

Coveney R. M. Jr., Leventhal J. S., Glascock M. D., and Hatch J. R. (1987) Origins of metals and organic matter in the Mecca Quarry Shale member and stratigraphically equivalent beds across the Midwest. *Econ. Geol.* **82,** 915–933.

Coyle C. L., Harmer M. A., George G. N., Daage M., and Stiefel E. I. (1992) Conversion of $[MoS_4]$ $[Mo_2S_2(\mu\text{-}S)_2S_2)_2]^{2-}$ to $[MoS_4]$ $[Mo_2S_2(\mu\text{-}S)_2S_2)_2]^{2-}$ by organic disulfides: The mechanism of an induced redox reaction. *Inorg. Chem.* **29,** 14–19.

Crusius J., Pedersen T. F., and Calvert S. E. (1999) A 36 kyr geochemical record from the Sea of Japan of organic matter flux variations and changes in intermediate water oxygen concentrations. *Paleoceanography* **14,** 248–259.

Dean W. E., Gardner J. V., and Piper D. Z. (1997) Inorganic geochemical indicators of glacial-interglacial changes in productivity and anoxia on the California continental margin. *Geochim. Cosmochim. Acta* **61,** 4507–4518.

Dean W. E., Piper D. Z., and Peterson L. C. (1999) Molybdenum accumulation in Cariaco basin sediment over the past 24 k.y: A record of water-column anoxia and climate. *Geology* **27,** 507–510.

Dellwig O., Böttcher M. E., Lipinski M., and Brumsack H.-J. (2002) Trace metals in Holocene coastal peats and their relation to pyrite formation (NW Germany). *Chem. Geol.* **182,** 423–442.

Draganjac M., Simhon E., Chan L. T., Kanatzidis M., Baenziger N. C., and Coucouvanis D. (1982) Synthesis, interconversions, and structural characterization of the $[(S_4)_2MoS]$ $[(S_4)_2MoO]^{2-}$, $[(S_4)_2MoS]$ $[(S_4)_2MoO]^{2-}$, $(Mo_2S_{10})^{2-}$, and $(Mo_2S_{12})^{2-}$ anions. *Inorg. Chem.* **21,** 3321–3332.

Erickson B. E. (1998) The speciation of molybdenum in sulfidic natural waters. Ph.D. dissertation. University of Maryland, College Park.

Erickson B. E. and Helz G. R. (2000) Molybdenum(VI) speciation in sulfidic waters: Stability and lability of thiomolybdates. *Geochim. Cosmochim. Acta* **64,** 1149–1158.

Giggenbach W. F. (1972) Optical spectra and equilibrium distribution of polysulfide ions in aqueous solution at 20°. *Inorg. Chem.* **11,** 1201–1207.

Giggenbach W. F. (1974) Equilibria involving polysulfide ions in aqueous sulfide solutions up to 240°. *Inorg. Chem.* **13,** 1724–1730.

Goldberg S., Su C., and Forster H. S. (1998) Sorption of molybdenum on oxides, clay minerals and soils. In *Adsorption of Metals by Geomedia* (ed. E. A. Jenne), chap 19. Academic Press.

Hadjikyriacou A. I. and Coucouvanis D. (1987) New members of the $[Mo_2(S)_n(S_2)_{6-n}]$ $[Mo_2S_9]$ $[Mo_2S_7]$ $[Mo_2S_6]^{2-}$ series. Synthesis, structural characterization and properties of the $[Mo_2(S)_n(S_2)_{6-n}]$ $[Mo_2S_9]$ $[Mo_2S_7]$ $[Mo_2S_6]^{2-}$, $[Mo_2(S)_n(S_2)_{6-n}]$ $[Mo_2S_9]$ $[Mo_2S_7]$ $[Mo_2S_6]^{2-}$, and $[Mo_2(S)_n(S_2)_{6-n}]$ $[Mo_2S_9]$ $[Mo_2S_7]$ $[Mo_2S_6]^{2-}$. *thio anions. Inorg. Chem.* **26,** 2400–2408.

Halbert T. R., Hutchings L. L., Rhodes R., and Stiefel E. I. (1986) Induced redox reactivity of tetrathiovanadate(V): Synthesis of the vanadium(IV) dimer $V_2(\mu\text{-}S)_2(i\text{-}Bu_2NCS_2)_4$ and its structural relationship to the V/S mineral patronite. *J. Am. Chem. Soc.* **108,** 6437–6438.

Harmer M. A. and Sykes A. G. (1980) Kinetics of the interconversion of sulfido- and oxomolybdate(VI) species $MoO_xS_{4-x}^{2-}$ in aqueous solutions. *Inorg. Chem.* **19,** 2881–2885.

Harmer M. A., Halbert T. R., Pan W.-H., Coyle C. L., Cohen S. A., and Stiefel E. I. (1986) Ligand and induced internal redox processes in Mo- and W-S systems. *Polyhedron* **5,** 341–347.

Helz G. R., Miller C. V., Charnock J. M., Mosselmans J. F. W., Pattrick R. A. D., Garner C. D., and Vaughan D. J. (1996) Mechanism of molybdenum removal from the sea and its concentration in black shales: EXAFS evidence. *Geochim. Cosmochim. Acta* **60,** 3631–3642.

Hibble S. J., Feaviour M. R., and Almond M. J. (2001) Chemical excision from amorphous $MoS_3$; a quantitative EXAFS study. *J. Chem. Soc. Dalton* **2001,** 935–940.

Huerta-Diaz M. G. and Morse J. W. (1992) Pyritization of trace metals in anoxic marine sediments. *Geochim. Cosmochim. Acta* **56,** 2681–2702.

LaMer V.K. and Dinegar R. H. (1950) Theory, production and mechanism of formation of monodispersed hydrosols. *J. Am. Chem. Soc.* **72,** 4847–4854.

Luther G. W. III, Giblin A. E., and Varsolona R. (1985) Polarographic analysis of sulfur species in marine porewaters. *Limnol. Oceanogr.* **30,** 727–736.

Mascharak P. K., Papaefthymiou G. C., Armstrong W. H., Foner S., Frankel R. B., and Holm R. H. (1983) Electronic properties of single and double- $MoFe_3S_4$ cubane type clusters. *Inorg. Chem.* **22,** 2851–2858.

McConnachie C. A. and Stiefel E. I. (1999) Ligand and tetrathiometalate effects in induced internal electron transfer reactions. *Inorg. Chem.* **38,** 964–972.

McKenzie R. M. (1983) The adsorption of molybdenum on oxide surfaces. *Aust. J. Soil Res.* **21,** 505–513.

Morford J. L. and Emerson S. (1999) The geochemistry of redox sensitive trace metals in sediments. *Geochim. Cosmochim. Acta* **63,** 1735–1750.

Müller A. (2002) Pyritization of iron and trace metals in anoxic fjord sediments (Nordåsvannet fjord, western Norway). *Appl. Geochem.* **17,** 923–934.

Müller A., Nolte W.-O., and Krebs B. (1978) $[(S_2)_2Mo(S_2)_2Mo(S_2)_2]^{2-}$, a novel complex containing only $S_2^{2-}$ ligands and a Mo-Mo bond. *Angew. Chem. Int. Ed. Engl.* **17,** 279.

Müller A., Krickemeyer E., Wittneben V., Bögge H., and Lemke M. (1991) $(NH_4)_2[Re_2S_{16}]$, a soluble metal sulfide with interesting electronic properties and unusual reactivity. *Angew. Chem. Int. Ed. Engl.* **30,** 1512–1514.

Murray H. H., Wei L., Sherman S. E., Greaney M. A., Eriksen K. A., Carstensen B., Halbert T. R., and Stiefel E. I. (1995) Induced internal electron transfer chemistry in rhenium sulfide systems. *Inorg. Chem.* **34,** 841–853.

Nameroff T. J., Balistrieri L. X., and Murray J. W. (2002) Suboxic trace metal geochemistry in the eastern tropical North Pacific. *Geochim. Cosmochim. Acta* **66,** 1139–1158.

Nesbitt H. W. and Muir I. J. (1994) X-ray photoelectron spectroscopic study of a pristine pyrite surface reacted with water vapour and air. *Geochim. Cosmochim. Acta* **58,** 4467–4679.

Osterloh F., Segal B. M., Achim C., and Holm R. H. (2000) Reduced mono-, di-, and tetracubane-type clusters containing the $[MoFe_3S_4]^{2+}$ core stabilized by tertiary phosphine ligation. *Inorg. Chem.* **39,** 980–989.

Pan W.-H., Leonowicz M. E., and Stiefel E. I. (1983) Facile syntheses of new molybdenum and tungsten sulfido complexes: Structure of $Mo_3S_9^{2-}$. *Inorg. Chem.* **22,** 672–678.

Raiswell R. and Plant J. (1980) The incorporation of trace elements into pyrite during diagenesis of black shales, Yorkshire, England. *Econ. Geol.* **75,** 684–699.

Shea D. and Helz G. R. (1988) The solubility of copper in sulfidic waters: Sulfide and polysulfide complexes in equilibrium with covellite. *Geochim. Cosmochim. Acta* **52,** 1815–1825.

Shea D. and MacCrehan W. A. (1988) Role of biogenic thiols in the solubility of sulfide minerals. *Sci. Total Environ.* **73,** 135–141.

Sugawara K., Okabe S., and Tanaka M. (1961) Geochemistry of molybdenum in natural waters (II). *J. Earth Sci. Nagoya Univ.* **9,** 114–128.

Vorlicek T. P. (2002) Toward a better understanding of molybdenum fixation in sediments: The roles of mineral catalysis, zero-valent sulfur, and metal sulfides. Ph.D. dissertation. University of Maryland, College Park.

Vorlicek T. P. and Helz G. R. (2002) Catalysis by mineral surfaces: Implications for Mo geochemistry in anoxic environments. *Geochim. Cosmochim. Acta* **66,** 3679–3692.

Wagman D. D., Evans W. H., Parker V. B., Schumm R. H., Halow I., Bailey S. M., Churney K. L., and Nuttal R. L. (1982) The NBS tables of chemical thermodynamic properties. *J. Phys. Chem. Ref. Data* **11 (***Suppl. 2***),** 392.

Wang F., Tessier A., and Buffle J. (1998) Voltammetric determination of elemental sulfur in pore waters. *Limnol. Oceanogr.* **43,** 1353–1361.

Yarincik K. M., Murray R. W., Lyons T. W., Peterson L. C., and Haug G. H. (2000) Oxygenation history of bottom waters in the Cariaco basin, Venezuela, over the past 578,000 years. Results from redox-sensitive metals (Mo, V, Mn, Fe). *Paleoceanography* **15,** 593–604.

Zheng Y., Anderson R. F., Van Geen A., and Kuwabara J. (2000a) Authigenic molybdenum formation in marine sediments: A link to pore water sulfide in the Santa Barbara Basin. *Geochim. Cosmochim. Acta* **64,** 4165–4178.

Zheng Y., van Geen A., Anderson R. G., Gardner J. V., and Dean W. E. (2000b) Intensification of the northeast Pacific oxygen minimum zone during the Bolling-Allerod warm period. *Paleoceanography* **15,** 528–536.